CAUSALITY AND RESPONSE THEORY

Denis J. Evans and Debra J. Searles

Research School of Chemistry, Australian National University
GPO Box 414, Canberra, A.C.T., 2601, Australia

We live in a universe where cause precedes effect. This is in spite of the fact that the equations of motion, whether classical or quantum mechanical, are time reversible and it is therefore dynamically possible for effect to precede cause. In our attempts to model the macroscopic behaviour of the world around us, we describe apparently irreversible behaviour such as heat or momentum flows, by using causal constitutive relations.

In the 1950's and 60's 'exact' fluctuation relations - the so-called Green-Kubo relations - were derived for the causal transport coefficients that are defined by causal linear constitutive relations such as Fourier's Law of heat flow or Newton's Law of viscosity [1-4]. The Mori-Zwanzig projection operator formalism shows that the Green-Kubo relations for causal linear transport coefficients are an exact consequence of the equations of motion. Some years ago an objection to the derivation of Green-Kubo relations by linear response theory was raised by van Kampen [5]. However, this objection has more recently been dismissed by Morriss et al. [6]

It would thus seem that the derivation of Green-Kubo relations, which give a unique sign for each of the Navier-Stokes transport coefficients, constitutes a proof of the irreversibility of macroscopic behaviour. Although Green-Kubo relations do not indicate the sign of the transport coefficient, they do indicate that the transport coefficient has a definite sign.

Recently we have provided a simple argument that if a deterministically and reversibly thermostatted system which is initially at equilibrium is subjected to a perturbing external field, then it becomes overwhelmingly probable to observe initial equilibrium microstates that subsequently generate Second Law satisfying nonequilibrium steady states [7]. This argument is based on the Boltzmann ansatz (that in the equilibrium microcanonical ensemble the probability of observing microstates within a specified phase space volume is proportional to the magnitude of that volume), and on the assumption of causality.

In this paper we show that if we derive Green-Kubo relations for the corresponding transport coefficients defined by *anticausal* constitutive relations: firstly, these anti-transport coefficients have the opposite sign to their causal counterparts and secondly, it becomes overwhelmingly likely to observe Second Law violating anticausal nonequilibrium steady states. This argument, again based on the Boltzmann ansatz, shows that in an anticausal world it becomes overwhelmingly probable to observe *final* equilibrium microstates that evolved from Second Law violating nonequilibrium steady states. Although this behaviour is not seen in the macroscopic world, *anticausal* behaviour is permitted by the solution of the time reversible laws of dynamics and we demonstrate, using computer simulation, how to find phase space trajectories which exhibit *anticausal* behaviour.

To make this discussion more concrete we will discuss Green-Kubo relations for shear viscosity [1]. Analogous results can be derived for each of the Navier-Stokes transport coefficients. We assume that the regression of fluctuations in a system at equilibrium, whose constituent particles obey Newton's equations of motion, are governed by the Navier-Stokes equations.

The causal response of the yx-component of the pressure tensor in the zero wavevector limit is given by,

$$P_{yxC}(t) = -\int_0^t \eta(t-s)\gamma(s)ds \qquad t > 0. \tag{1}$$

and the anticausal response is,

$$P_{yxA}(t) = \int_t^0 \eta(t-s)\gamma(s)ds \qquad t<0 \tag{2}$$

The Green-Kubo expression for the *causal* shear viscosity coefficient can be evaluated using standard techniques [1]. We have recently derived the *anticausal* shear viscosity coefficient in a similar manner [10]. At zero wavevector, we find that the causal and anticausal memory functions are both given by the equilibrium autocorrelation function of the pressure tensor,

$$\eta(t) = \frac{V}{k_B T}\left\langle P_{yx}(t)P_{yx}(0)\right\rangle, \quad \forall t \tag{3}$$

where $t > 0$ for the causal response and $t < 0$ for the anticausal response.

In the linear regime close to equilibrium the entropy production per unit time, dS/dt, is given by,

$$\frac{dS}{dt} = -P_{yx}(t)\gamma(t)V \tag{4}$$

where $\gamma(t)$ is the time dependent strain rate. From equations (1) and (2), it is easy to see that if we conduct two shearing experiments, one on a causal system with a strain rate history $\gamma_C(t)$ and one on an anticausal system with $\gamma_A(t) = \pm\gamma_C(-t)$, then

$$\left.\frac{dS(t)}{dt}\right|_A = \left.\frac{-dS(-t)}{dt}\right|_C \tag{5}$$

This proves that if the causal system satisfies the Second Law of Thermodynamics then the anticausal system must violate that Law and vice versa [10].

We can examine the causal and anticausal response at the microscopic level by considering a thermostatted system of N particle under shear. In this system the field is the shear rate, $\partial u_x/\partial y = \gamma(t)$ (the y-gradient of the x-streaming velocity), and the dissipative flux is the shear stress, $-P_{xy}$, times the system volume, V [1]. The equations of motion for the particles are given by the the so-called thermostatted SLLOD equations [1],

$$\dot{\mathbf{q}}_i = \mathbf{p}_i/m + i\gamma y_i, \quad \dot{\mathbf{p}}_i = \mathbf{F}_i - i\gamma p_{yi} - \alpha \mathbf{p}_i. \tag{6}$$

At arbitrary strain rates these equations give an exact description of adiabatic Couette flow. At low Reynolds number, the momenta, $\mathbf{p}_i$, are peculiar momenta and α is determined using Gauss's Principle of Least Constraint to keep the internal energy fixed [1]. Thus

$$\alpha = -\gamma[\sum_{i=1}^{N} p_{xi}p_{yi}/m - 1/2\sum_{i,j}^{N} x_{ij}F_{yij}]/\sum_{i=1}^{N}\mathbf{p}_i^2/m = -P_{xy}\gamma V/\sum_{i=1}^{N}\mathbf{p}_i^2/m \tag{7}$$

where F_{yij} is the y-component of the intermolecular force exerted on particle i by j and $x_{ij} \equiv x_j - x_i$. Note that the thermostatted SLLOD equations of motion (6 and 7) are time reversible [1].

We have shown that for every i-segment with τ-averaged shear stress $\langle P_{xy}\rangle_{\tau,(i)} \equiv \frac{1}{\tau}\int_0^\tau P_{xy}(\Gamma_{(i)}(s))ds$, there exists a conjugate segment which we will call the $i^{(K)}$ segment for which $\langle P_{xy}\rangle_{\tau,(i^{(K)})} = -\langle P_{xy}\rangle_{\tau,(i)}$ [7]. The K-mapping of a phase, Γ, is defined by $M^K\Gamma = M^K(x,y,z,p_x,p_y,p_z,\gamma) = (x,-y,z,-p_x,p_y,-p_z,\gamma) \equiv \Gamma^{(K)}$ [1]. It is straightforward to show that the Liouville operator for the system (6 and 7), $iL(\Gamma,\gamma) \equiv \sum[\dot{\mathbf{q}}_i \cdot \partial/\partial\mathbf{q}_i + \dot{\mathbf{p}}_i \cdot \partial/\partial\mathbf{p}_i]$, has the property that under a K-map, $M^K\, iL(\Gamma,\gamma) = iL(\Gamma^{(K)},\gamma) = -iL(\Gamma,\gamma)$ [1], from which it follows that if a K-map is carried out at $t = 0$, and if, $\gamma_K(-t) = \gamma(t) \quad \forall t$, then.

$$P_{xy}(-t,\Gamma,\gamma(-t)) = \exp[-iL(\Gamma,\gamma(-t))t]P_{xy}(\Gamma) = -P_{xy}(t,\Gamma^{(K)},\gamma_K(t)) \tag{8}$$

If we select an initial, $t = 0$, phase, $\Gamma_{(1)}$, and we advance time from 0 to τ using the equations of motion (6 and 7), we obtain $\Gamma_{(2)} = \Gamma(\tau;\Gamma_{(1)}) = \exp[iL(\Gamma_{(1)},\gamma)\tau]\Gamma_{(1)}$. Continuing on to 2τ gives $\Gamma_{(3)} = \exp[iL(\Gamma_{(2)},\gamma)\tau]\Gamma_{(2)} = \exp[iL(\Gamma_{(1)},\gamma)2\tau]\Gamma_{(1)}$. At the *midpoint* of the trajectory segment $\Gamma_{(1,3)}$ (i.e. at $t = \tau$) we apply the K-map to $\Gamma_{(2)}$ generating $M^{(K)}\Gamma_{(2)} \equiv \Gamma_{(5)}$. If we now reverse time with the

same shear rate (but with a reversed evolution), we obtain $\Gamma_{(4)} = \exp[-iL(\Gamma_{(5)},\gamma)\tau]\Gamma_{(5)}$. $\Gamma_{(4)}$ is the initial t = 0 phase from which a segment $\Gamma_{(4,6)}$ can be generated with $\Gamma_{(6)} = \exp[iL(\Gamma_{(4)},\gamma)2\tau]\Gamma_{(4)}$. We thus have an algorithm for generating conjugate segment pairs [7].

Using the symmetry of the equations of motion it is trivial to show that $P_{xy}(t; \Gamma_{(1)}, 0 < t < 2\tau) = -P_{xy}(2\tau-t; \Gamma_{(6)}, 0 < t < 2\tau)$. We also see immediately that if the segment $\Gamma_{(1,3)}$ is a causal segment then segment $\Gamma_{(4,6)}$ is anticausal, and vice versa. Further, if segment $\Gamma_{(1,3)}$ is a Second Law satisfying segment then segment $\Gamma_{(4,6)}$ is a Second Law violating segment, and vice versa. Figure 1 below shows computer simulation generated results showing causal and anticausal conjugate segments.

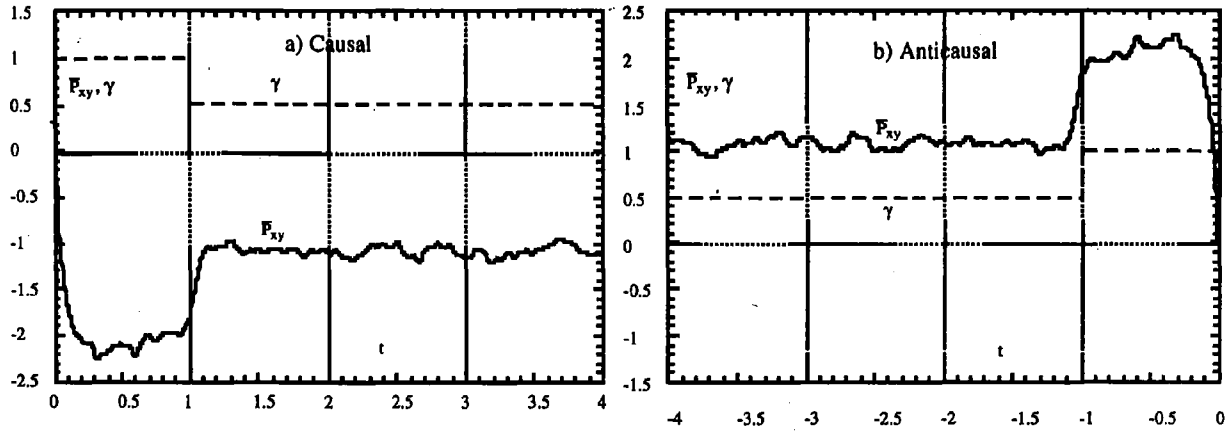

Figure 1a,b. $\overline{P}_{xy}$ *(solid line) from nonequilibrium molecular dynamics simulations of 56 WCA particles at T = 1.0 and n = 0.8 undergoing shear flow. The dashed line gives the time dependence of the strain rate. In a),* $\overline{P}_{xy}$ *was determined using 100 trajectories whose initial phases were selected from an equilibrium distribution and to which a two step strain rate was applied. b) shows* $\overline{P}_{xy}$ *for their conjugate trajectories. The conjugate trajectories were obtained by applying a K-map to the phase of the trajectory at t =2, simulating forward and backward in time from this point and translating in time so that the conjugate trajectory ends at t = 0 . Note that the strain rate history of the conjugate trajectory is reversed.*

In a causal world, which is described by causal macroscopic constitutive relations, observed segments are overwhelmingly likely to be Second Law satisfying. We can show this by discussing the ratio of probabilities of finding the initial phases $\Gamma_{(1)}$, $\Gamma_{(4)}$ which generate these conjugate segments. In a causal world, the probabilities of observing the segments $\Gamma_{(1,3)}$ and $\Gamma_{(4,6)}$ ($p_{(1,3)}$,$p_{(4,6)}$) are of course proportional to the probabilities of observing the *initial* phases which generate those segments. It is convenient to consider a small phase space volume, $V(\Gamma_{(i)}(0))$ about an initial phase, $\Gamma_{(i)}(0)$. Because the initial phases are distributed *microcanonically*, the probability of observing ensemble members inside $V(\Gamma_{(i)}(0))$, is proportional to $V(\Gamma_{(i)}(0))$. From the Liouville equation $df(\Gamma,t)/dt = 3N\alpha(\Gamma)f(\Gamma,t) + O(1)$ and the fact that for sufficiently small volumes, $V(\Gamma(t)) \sim 1/f(\Gamma(t),t)$, we can make the following observations: $V_2 = V_1(\tau) = V_1(0)\exp[-\int_0^\tau 3N\alpha(s;\Gamma_{(1)})ds]$ and $V_3 = V_1(2\tau) = V_1(0)\exp[-\int_0^{2\tau} 3N\alpha(s;\Gamma_{(1)})ds]$; and since the Jacobian of the K-mapping is unity, $V_2 = V_5$, $V_3 = V_4$ and $V_1(0) = V_6$. Therefore the ratio of probabilities is just the volume ratio,

$$p_{(4,6)}/p_{(1,3)} = V_4/V_1(0) = V_1(2\tau)/V_1(0) = \exp[\int_0^{2\tau} -3N\alpha(s;\Gamma_{(1)})ds], \quad \forall\tau. \qquad (9)$$

Thus if the world is causal and we assume segment $1(\equiv\Gamma_{(1,3)})$ is Second Law satisfying then $\langle\alpha\rangle_{\tau,(1,3)} > 0$ and $\mu_1/\mu_{1*}\to\infty$ (i.e. we overwhelmingly observe segment 1 rather than the Second Law violating antisegment 1*). Conversely, if segment 1 is Second Law violating then $\langle\alpha\rangle_{\tau,(1,3)} < 0$ and $\mu_1/\mu_{1*}\to 0$ (i.e. we overwhelmingly see segment 1* rather than the Second Law violating antisegment 1).

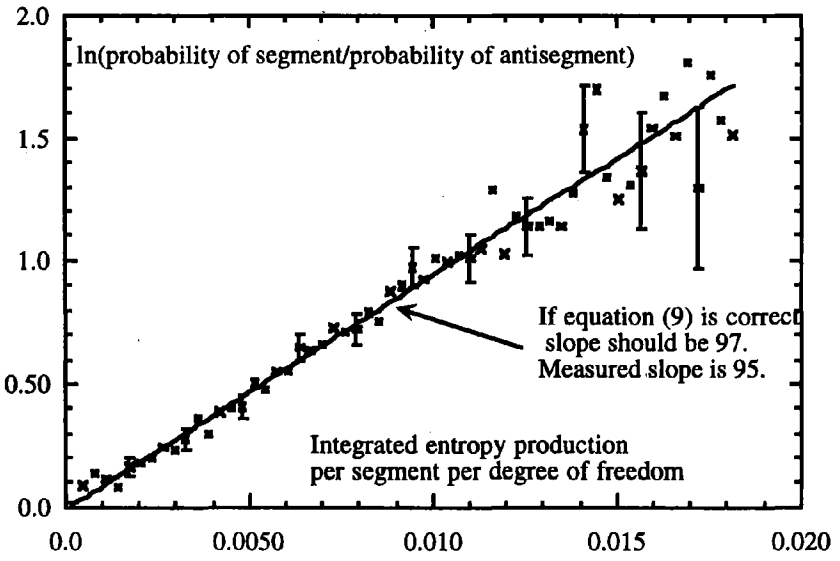

Figure 2. *Shows results[7] of a computer simulation test of the validity of (9).*

In an anticausal world where effects precede their causes, the probabilities of observing the segments $\Gamma_{(1,3)}, \Gamma_{(4,6)}$ are proportional to the probabilities of observing the *final* phases generated by those segments. The system will be at equilibrium at the end point (rather than the beginning) of the trajectory segments and antisegments. It is trivial to see that in an anticausal world it would be overwhelmingly more probable to observe Second Law violating segments rather than Second Law satisfying segments.

These relationships between causality, response theory and the second law of thermodynamics have been demonstrated using nonequilibrium molecular dynamics simulations of Couette flow in [10].

Acknowledgement

DJE would like to thank the National Institute of Standards and Technology for partial support of this work. DJS would like to thank the Australian Research Council for the award of an ARC Fellowship.

References

[1] D. J. Evans and G. P. Morriss, *Statistical Mechanics of Nonequilibrium Liquids* (Academic Press, London, 1990).
[2] M. S. Green, J. Chem. Phys. **22**, 398 (1954).
[3] R. Kubo, J. Phys. Soc. Japan **12**, 570 (1957).
[4] R. Zwanzig, Ann. Rev. Phys. Chem. **16**, 67 (1965).
[5] N. G. van Kampen, Phys. Norvegica **5**, 279 (1971).
[6] G. P. Morriss, D. J. Evans, E. G. D. Cohen and H. van Beijeren, Phys. Rev. Lett. **62**, 1579 (1989).
[7] D. J. Evans and D. J. Searles, Phys. Rev. E **50**, 1645 (1994).
[8] A. B. Pippard, *Response and Stability: An Introduction to the Physical Theory* (Cambridge University Press, Cambridge, 1985).
[9] J. D. Weeks, D. Chandler and H. C. Andersen, J. Chem. Phys. **54**, 5237 (1971).
[10] D. J. Evans and D. J. Searles, Phys. Rev. E. submitted (1995).